2019-02-13

Developable Mechanisms on Developable Surfaces

Todd G. Nelson
Brigham Young University - Provo, toddgn@gmail.com

Trent K. ZImmerman
Brigham Young University - Provo, trentzim@gmail.com

Robert J. Lang
Lang Origami, robert@langorigami.com

Spencer P. Magleby
Brigham Young University - Provo, magleby@byu.edu

Larry L. Howell
Brigham Young University - Utah, lhowell@byu.edu

Original Publication Citation

Nelson, T., Zimmerman, T., Magleby, S., Lang, R., and Howell, L., "Developable Mechanisms on Developable Surfaces," Science Robotics, Vol. 4, Issue 2, DOI: 10.1126/scirobotics.aau5171, 2019.

FRONT MATTER

Developable mechanisms on developable surfaces

Todd G. Nelson[1], Trent K. Zimmerman[2], Spencer P. Magleby[2], Robert J. Lang[3], Larry L. Howell[2]*

The trend toward smaller mechanism footprints and volumes, while maintaining the ability to perform complex tasks, presents the opportunity for exploration of hypercompact mechanical systems integrated with curved surfaces. Developable surfaces are shapes that a flat sheet can take without tearing or stretching, and they represent a wide range of manufactured surfaces. This work introduces "developable mechanisms" as devices that emerge from or conform to developable surfaces. They are made possible by aligning hinge axes with developable surface ruling lines to enable mobility. Because rigid-link motion depends on the relative orientation of hinge axes and not link geometry, links can take the shape of the corresponding developable surface. Mechanisms are classified by their associated surface type, and these relationships are defined and demonstrated by example. Developable mechanisms show promise for meeting unfilled needs using systems not previously envisioned.

INTRODUCTION

There is a need for mechanical systems to be compact while still performing complex tasks. For example, instruments for minimally invasive surgery must be capable of sophisticated mechanical functions, but patient outcomes are improved by smaller incisions. Air vehicle flight time and ground vehicle fuel efficiency can be improved by motion and shape manipulation, but adding the corresponding mechanisms adds weight. Consumer expectations for electronic device performance demand ever-increasing capabilities without increasing volume. This paper introduces "developable mechanisms" to help address these conflicting requirements. These mechanisms have the ability to be contained within or conform to a developable surface in one of its configurations, as shown in Fig. 1A.

This class of mechanisms is derived from a synthesis of concepts from compliant mechanisms, origami-based mechanical systems, rigid-link kinematics, and developable surface geometry. Compliant mechanisms generate some or all their motion from flexing of their constituent components. This combination of form and function enables smaller mechanism packages with precise movements while reducing part count (*1*–*3*). Compact compliant mechanisms emerging from a plane or stacked planes have been studied as lamina-emergent mechanisms (LEMs) (*4*, *5*). Origami-based mechanical systems can be created from a two-dimensional (2D) sheet yet have sophisticated 3D motion (*6*, *7*). The deployment and stowing capabilities of origami-based systems, combined with the possibility of manufacturing and assembly from planar materials, can be exploited to address challenges requiring compact mechanism footprints and volumes (*8*–*12*). For example, compact minimally invasive surgical instruments and biomimetic devices have resulted from origami principles (*13*–*16*). The use of surfaces to generate complex mechanisms has also been investigated (*17*, *18*). Similarly, compact footprints and volumes may also be possible in systems with developable surfaces by integrating the mechanism with the surface. A developable surface results when a plane (such as a sheet of paper or metal) is deformed through bending, provided that no stretching or tearing occurs in the surface (*19*). These surfaces are composed of straight lines, called rulings or generators, that can be used to classify developable surfaces into four types: planes, generalized cylinders (parallel ruling lines), generalized cones (ruling lines intersect at a point called the apex or focal point), and tangent developables (ruling lines tangent to a space curve). General, or hybrid, developable surfaces are composed of two or more of the fundamental types joined in a surface that retains developability. Because of their compatibility with inexpensive manufacturing processes, combined with utility in a wide range of products from aircraft to clothing to appliances, modeling and fabrication of developable surfaces continue to be active areas of research (*20*, *21*).

We define developable mechanisms to be mechanisms that (i) are contained within or conform to developable surfaces when both are modeled with zero thickness, (ii) have mobility, and (iii) do not require the developable surface to deform to enable the mechanism's movement. The mobility of multiaxis, multilink developable mechanisms can be achieved by aligning hinge axes of linkages with ruling lines on developable surfaces. This alignment principle, combined with known fundamentals of mechanical systems and compliant mechanisms reviewed above, makes it useful to define this class of compact devices.

RESULTS

Definitions: Hinge axis ruling condition

Criteria (i) and (iii) illuminate conditions of the placement of revolute joint axes (hinge axes). Because hinge axes are straight line segments, for the axes to be contained in a developable surface, they need to be placed along ruling lines as shown in Fig. 1A. Similarly, for a mechanism to conform to a developable surface, the hinges need to be aligned to ruling lines in an offset developable surface when thickness is not negligible (see Fig. 1A). We call this condition the hinge axis ruling condition. For the conical developable surface shown in Fig. 1B, the hinge axis condition is illustrated by selecting hinge lines on rulings. The hinge axis condition could also apply to mechanisms placed on ruled, nondevelopable surfaces; however, we specifically address mechanisms on developable surfaces because of their compatibility with planar manufacturing. Although any type of joints that can be constrained to follow paths contained in the surface could be possible, this work focuses on revolute joints.

Definitions: Link shaping

Although satisfaction of the hinge axis ruling condition partially meets criterion (i), we draw upon a fundamental principle of linkage analysis to ensure that the mechanism links can be contained within or conform to a developable surface: The relative motion of rigid links is independent

[1]Department of Engineering, University of Southern Indiana, 8600 University Blvd, Evansville, IN 47712, USA. [2]Department of Mechanical Engineering, Brigham Young University, 435 CTB, Provo, UT 84602, USA. [3]Lang Origami, Alamo, CA 94507, USA. *Corresponding author. Email: lhowell@byu.edu

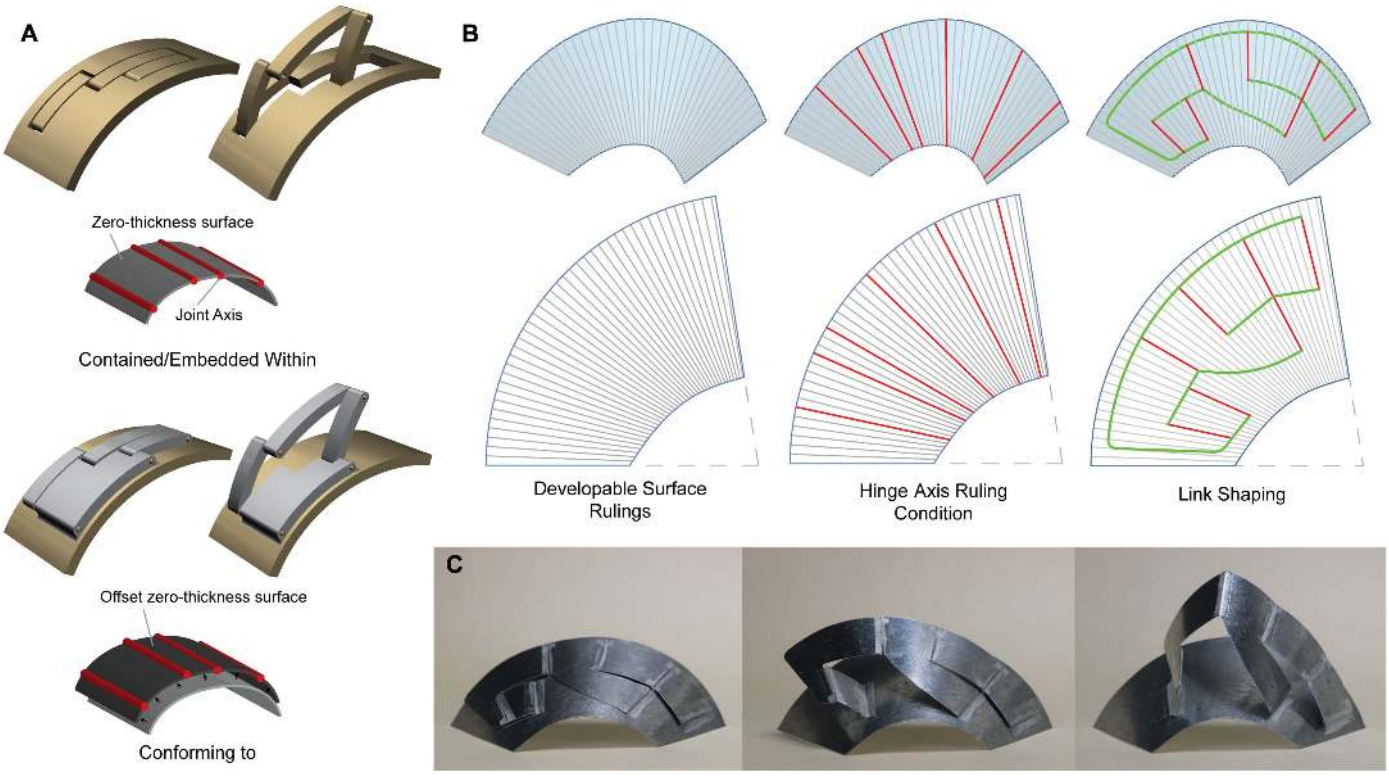

Fig. 1. Fundamental principles for constructing developable mechanisms. (**A**) Developable mechanisms can be contained within a developable surface where the joint axes are contained in the zero-thickness surface model or conform to a developable surface where the joint axes are on another developable surface that is offset from the surface to which it conforms. (**B**) The zero-thickness model for a generalized cone shown with its rulings both in a 3D state (top) and in a planar-developed state (bottom). Hinge axes and ruling lines are aligned according to the hinge axis ruling condition. Link shapes can be chosen to conform to the surface and connect hinge axes to appropriately create a mechanism. The pictured mechanism is a spherical linkage with six hinges (six bars). (**C**) A front view of a constructed spherical six-bar linkage conforming to a generalized cone with the mechanism in closed, partially open, and fully open states.

of link shapes as long as self-interference does not occur. Consequently, the links of a mechanism can take the shape of a developable surface. Figure 1B shows how link shapes can be chosen that conform to the surface and connect appropriately placed hinges. For example, for the single degree-of-freedom (DOF) spherical six-link mechanism placed on a cone in Fig. 1B, two of the links are tertiary links, meaning they connect three hinge axes. A physical prototype of a developable mechanism conforming to this surface was created in a 30-gauge (0.3 mm) galvanized steel sheet formed with a slip roller and 0.05-mm acrylic adhesive-backed polyethylene terephthalate (PET) hinges and is shown in Fig. 1C. The mechanism's motion is shown in Movie 1.

Analysis: Classification

The hinge axis ruling condition suggests a division of developable mechanisms into subclasses that correspond with the types of developable surfaces, which are categorized by their rulings. A developable mechanism with hinge axes that correspond to the ruling lines of a single type of developable surface can be subclassified as a planar, cylindrical, conical, or tangent developable mechanism. Hybrid developable mechanisms have hinge axes corresponding to ruling lines of two or more types of developable surfaces. Examples of the three curved subclasses of developable mechanisms are shown in Fig. 2. The identification of these developable mechanism subclasses enables linkage analysis to assess their motion characteristics.

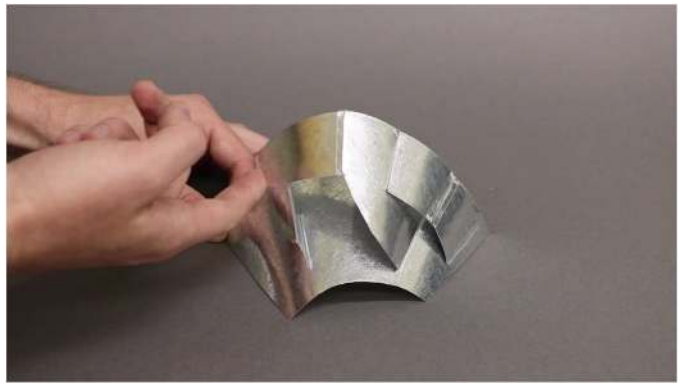

Movie 1. Movement of a conical developable mechanism conforming to a generalized cone.

Analysis: Mapping

Aligning hinge axes with ruling lines of generalized cylinders results in systems that can be modeled using established methods for planar mechanisms (*22*) and can draw upon principles from the body of work continually being developed (*23*–*25*). Figure 2A shows a right cylinder with a planar linkage skeleton in Fig. 2B that can be aligned to the ruling lines as shown in Fig. 2C. The physical realization of the mechanism in a closed position is depicted in Fig. 2D and in an open position in Fig. 2E. Details of this cylindrical developable mechanism's

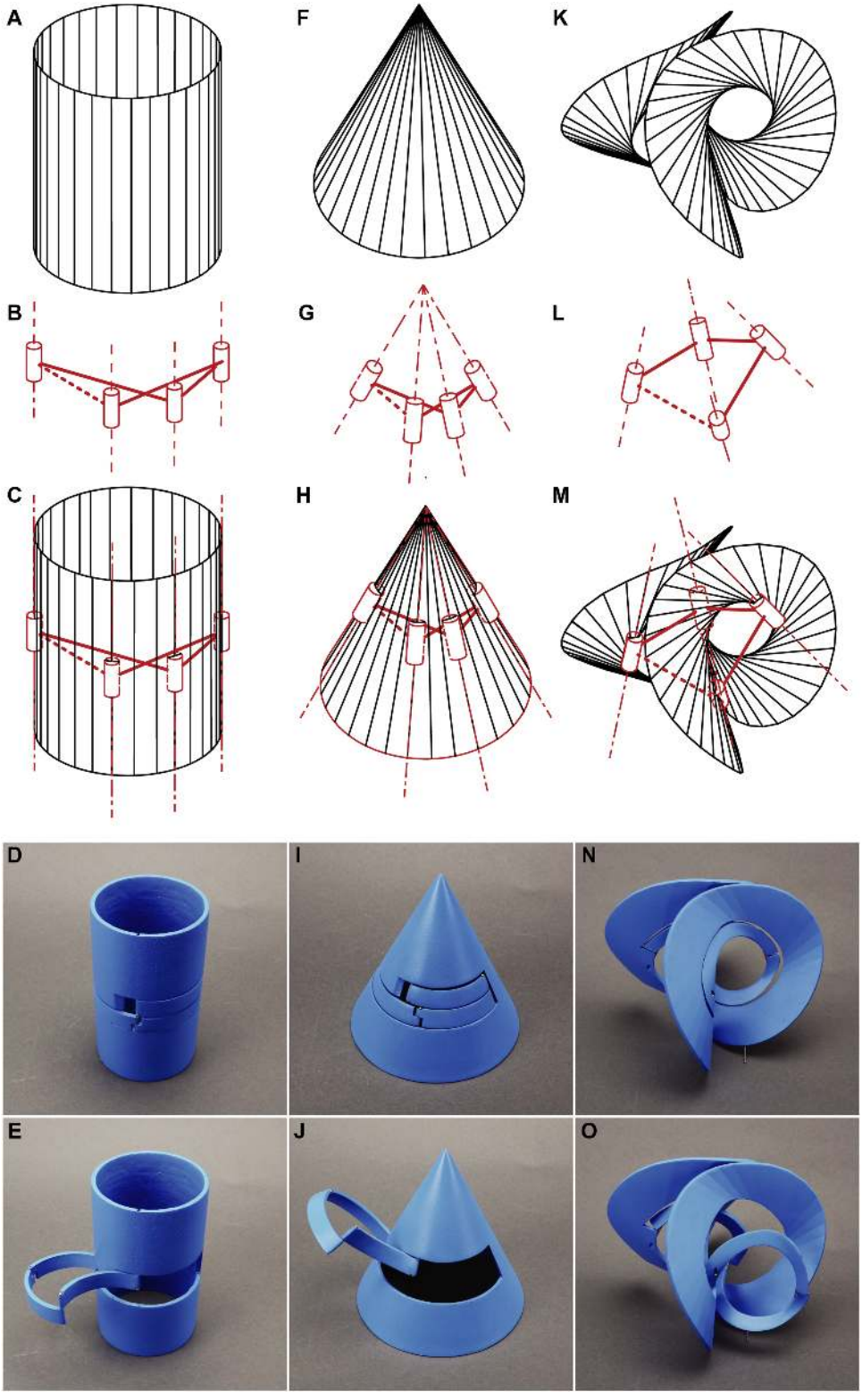

Fig. 2. The relationship between developable surfaces, mechanisms, and their corresponding developable mechanisms. From top to bottom by column, a surface type is followed by a corresponding mechanism class. Embedded and actuated configurations of physical developable mechanism prototypes are also shown. (**A** to **E**) A cylinder and planar mechanism make up a cylindrical developable mechanism. (**F** to **J**) A cone and spherical mechanism make up a conical developable mechanism. (**K** to **O**) A tangent developable surface and a Bennett mechanism make up a tangent developable mechanism.

design and construction are described in Supplementary Text and fig. S1.

Linkages with hinge axes that intersect at a point can be modeled as spherical mechanisms, drawing upon both established methods and recent spherical mechanism studies (*26*–*28*). Any point on the links of a spherical mechanism follows a path along a surface of a sphere. Consequently, placing hinge axes on the ruling lines of a generalized cone, as is required for a conical developable mechanism, results in a spherical mechanism. To illustrate this, we chose the ruling lines of the right cone in Fig. 2F as hinge axes, resulting in the spherical mechanism of Fig. 2G. The surface and linkage are superimposed in Fig. 2H. The physical realization of the mechanism in two positions is shown in Fig. 2 (I and J). Figure 2J also illustrates how the intersection point of the joint axes stays at the apex of the cone throughout the mechanism's movement. The conical developable mechanism's design is shown in Fig. 3, and the design steps will be discussed in a later section.

Linkages with nonintersecting hinge axes can be modeled as spatial mechanisms (*29*, *30*). Continuing advancements in the study of spatial mechanisms has enhanced the ability to produce complex mechanism motions (*31*, *32*). The space curve to which the rulings of a tangent developable surface are tangent is called the edge of regression (*33*), and given the variety of possible edge of regressions, tangent developables can have diverse appearances. Neglecting special cases of coplanar or coaligned ruling lines, placing linkage hinge axes on the ruling lines of a tangent developable surface results in a spatial mechanism. In Fig. 2K, a specific tangent developable is shown, whose axes correspond to the axes of a Bennett linkage, an overconstrained spatial mechanism (*34*, *35*), shown in Fig. 2L. Unlike for the cylindrical and conical developable mechanisms shown in Fig. 2, where the mechanism hinge axes could be placed on any of the ruling lines, this specific tangent developable surface was carefully chosen for the Bennett linkage to align with its ruling lines as shown in Fig. 2M. As will be discussed later, this condition for a specific surface can be relaxed for linkages with a higher number of links. The physical realizations of this mechanism in closed and open states are shown in Fig. 2 (N and O). Details for the design

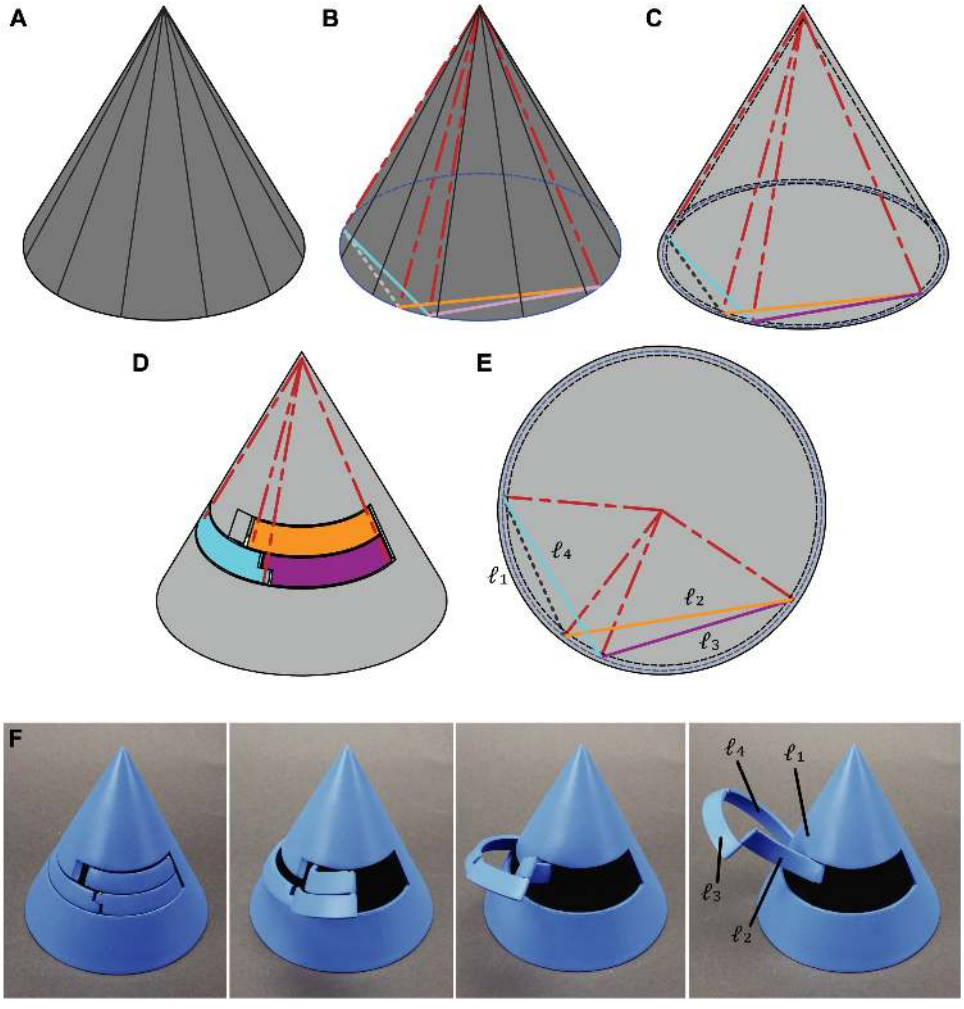

Fig. 3. Steps for the creation of a conical developable mechanism. (**A**) A cone is selected as the base surface for the mechanism. (**B**) Ruling lines with arbitrary positions that will serve as joint axes and the corresponding linkage skeleton are established. The joint axes are represented by center lines. The links are represented by solid lines with the exception of the dashed ground link (ℓ_1). (**C**) Thickness is added to the surface. (**D**) The links are fully modeled into the surface. Material is removed from the base surface near ℓ_2 to allow for a larger range of motion. (**E**) Skeleton links are labeled. (**F**) Various positions of a 3D-printed and assembled physical prototype are shown, beginning with the embedded position (left) and leading to the actuated (right) positions. Links labels correspond to those in the skeleton diagram.

and construction of this tangent developable mechanism are presented in Supplementary Text and figs. S2 and S3.

Planes can be assigned arbitrary rulings, provided that the lines do not cross each other, giving flexibility to the placement of hinge axes of a developable mechanism placed on a plane. Planar developable mechanisms have been previously studied under the names of LEMs and pop-up mechanisms (*36*, *37*). Because of the arbitrary nature of the ruling lines on a plane, planar developable mechanisms can consist of both planar and spherical linkages.

Analysis: Mobility

The mapping of developable mechanisms to planar, spherical, and spatial mechanisms can inform the conditions for mobility or criterion (ii). The mobility is the number of DOF or equivalently the number of inputs necessary to determine the position of all points on a mechanism. The Grübler-Kutzbach criterion (*22*), summarized in Supplementary Texts, predicts that any single-loop planar or spherical mechanism with only revolute or prismatic joints (each having a single DOF) must consist of at least four links to have mobility. The minimal constraints are used to illustrate cylindrical and conical developable mechanisms with four-link, four–revolute joint (4R) mechanisms shown in Fig. 2.

For a general single-loop spatial mechanism with single-DOF joints to have mobility, there must be at least seven links and joints. There exist, however, a few special case mechanisms that have mobility with fewer links, and You and Chen (*38*) listed these overconstrained mechanisms. Such mechanisms require conditions to be met that restrain the placement of the joint axes. Consequently, although these special case mechanisms can be made into developable mechanisms, the constraints force the surface to have ruling lines correlating to predetermined joint axes. There is only one known 4R overconstrained linkage that has mobility (*8*), the Bennett linkage (*34*, *35*), which is demonstrated in Fig. 2. The restrictions imposed on a developable surface by overconstrained linkages can be avoided by using 7R or higher single-loop linkages to accommodate arbitrary tangent developable surfaces. Although the Grübler-Kutzbach criterion predicts single-DOF mobility for a 7R loop, the range of motion for the links can be limited, and many singular points can exist.

Analysis: Parametric mathematical representation

For the four fundamental types of developable surfaces and ruled surfaces, the hinge axis ruling condition also leads to a straightforward way to mathematically relate revolute joint axes to the common parametric representation of the surface. This parametric representation has the general form of

$$\boldsymbol{s}(u, v) = \boldsymbol{\alpha}(u) + v\boldsymbol{\beta}(u) \quad (1)$$

where $\boldsymbol{\alpha}(u)$ is the directrix of the surface and $\boldsymbol{\beta}(u)$ are the directions of the rulings (*39*). Letting the parameter u be a constant reduces the parametric equation of the surface to the equation of a single ruling line. Therefore, n joint axes can be defined by constants u_i for $i = 1$ to n. The vector in the direction of the hinge axis, $\boldsymbol{z}_{i-1}$, will be simply $\boldsymbol{\beta}(u_i)$.

Analysis: Relating Denavit-Hartenberg parameters to developable surface geometry

It is common to represent both open and closed rigid-link spatial linkages using the Denavit-Hartenberg (DH) convention (*40*). Use

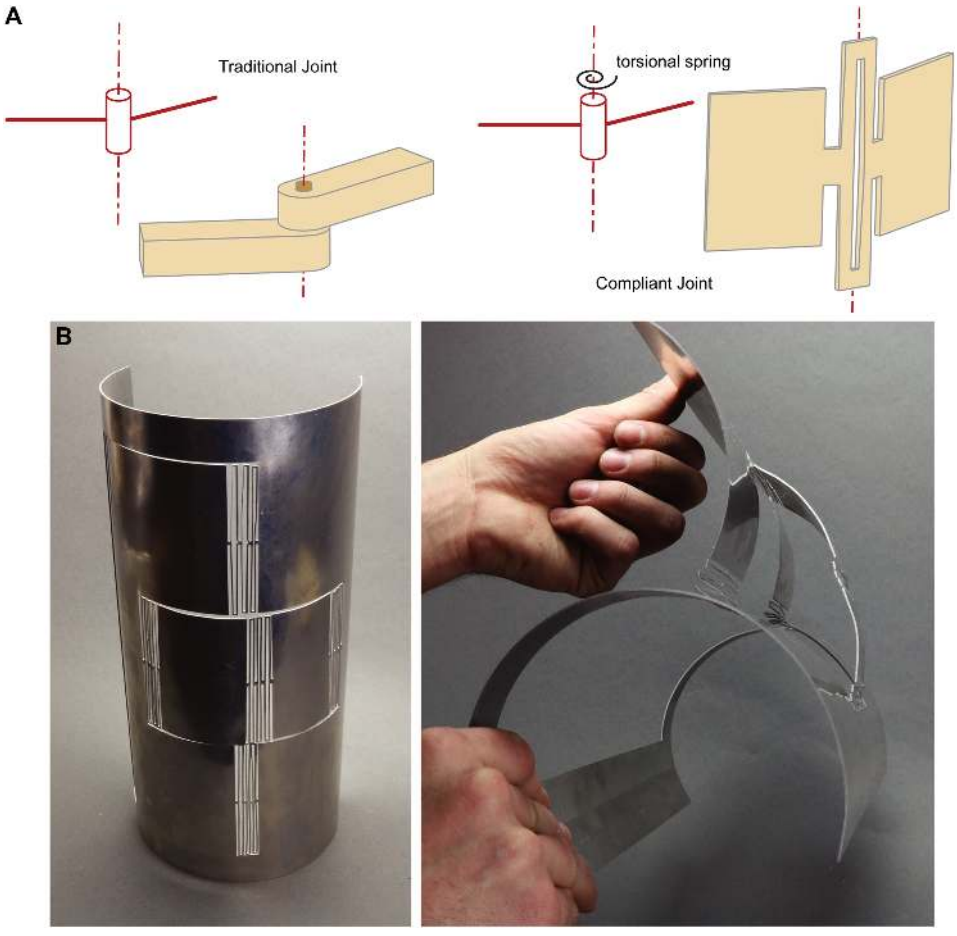

Fig. 4. Compliant joints and developable mechanisms. (**A**) Compliant flexures can be used in place of traditional hinges to further integrate the linkage into or onto a surface. (**B**) The stowed and deployed configurations of a compliant cylindrical developable mechanism. Useful mechanisms can be created with 2D manufacturing techniques to be later formed to the desired developable shape.

of this convention results in a consistent way to assign frames to links where only four parameters are needed to describe the transformation from one frame to another rather than the six parameters (three translations and three rotations) according to Euler's Rotation theorem for general transformations.

We can write the DH parameters of developable mechanisms using the geometry of the surface in which the mechanism is embedded. These DH parameters provide a way to write loop-closure equations for analyzing the motion of closed-chain linkages or to compute the forward kinematics of open-chain mechanisms. We see that, for cylindrical developable mechanisms and conical developable mechanisms, two of the four DH parameters are always zero. In addition, we create expressions for joint offsets to ensure that the joint angles are zero for the position where the mechanism is aligned with the surface. Details of determining the DH parameters and joint offsets using the surface geometry are presented in Materials and Methods.

Realization: Possible design methods

Although multiple methods to design a developable mechanism may be possible, one sequence of steps for creating a developable mechanism on a single type of developable surface is summarized here and illustrated in Fig. 3.

1) Select a specific zero-thickness surface in which a mechanism will be placed or an offset developable surface conforming to the surface on which the mechanism will be fit. Figure 3A shows a cone selected as the surface in which a mechanism will be placed.

2) Choose the ruling lines that will serve as joint axes. Figure 3B shows ruling lines on a cone that have been selected as joint axes and the linkage skeleton chosen.

3) Analyze the motion of the linkage skeleton using DH parameters computed from the surface and joint axes or other kinematic analysis methods.

4) Apply thickness to the zero-thickness–modeled surfaces. Figure 3C shows how thickness is applied symmetrically about the zero-thickness surface in preparation for an embedded developable mechanism.

5) Using the results from the previous steps, define link shapes that avoid interference and ensure that the links are contained within or conform to the surface. Figure 3D shows the link shapes chosen for a conical developable mechanism. Figure 3 (E and F) shows the links of the mechanism skeleton labeled and a 3D-printed prototype of the mechanism, respectively.

We further demonstrate this design approach through embedding an approximate straight line linkage into a right cylinder as described in Materials and Methods.

Realization: Incorporating flexures into developable mechanisms

Whereas traditional pin hinges or bearings present possible ways to construct developable mechanisms, flexures can further integrate form and function. As shown in Fig. 4A, flexures can be approximated as hinges at appropriate locations with torsion springs to represent their resistance to motion [i.e., a pseudo-rigid body model (*41*–*43*)]. Thus, hinges of developable mechanisms can be replaced by flexures, enabling monolithic developable mechanisms that are made from the surface itself. The flexures can be incorporated into a planar material before it is formed into a 3D shape or after forming has taken place (the strategy of designing elements of a developable mechanism before forming the surface is discussed further in Supplementary Text). These joints can take a variety of forms, such as small-length flexural pivots and lamina emergent torsional (LET) joints (*44*). Figure 4B shows a developable mechanism where a series of LET joints were water-jet cut into a flat metal sheet, which was then formed into the cylindrical shape shown. In addition, Fig. 4B shows the resulting four-link developable mechanism moved from its closed position to an open position. Further details of the design of this mechanism are included in Supplementary Texts and figs. S4 and S5. Flexures can also be formed from thin materials that can conform to the surface,

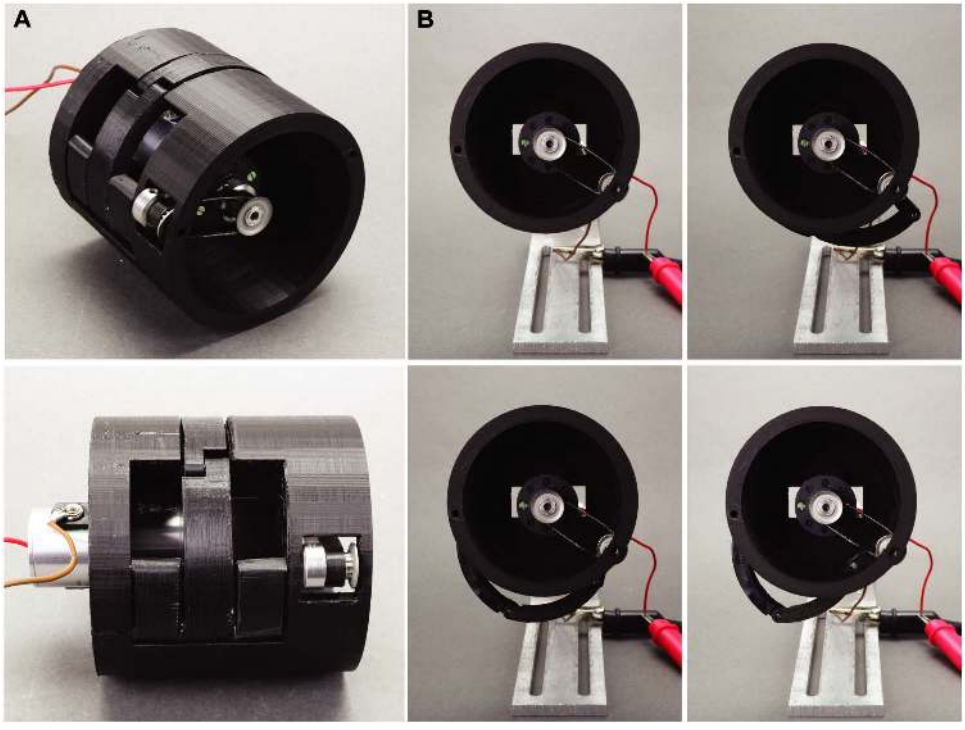

Fig. 5. Motorized cylindrical developable mechanism. (**A**) A motorized, fully revolving linkage emerging from a cylinder that results in a walking motion. (**B**) A sequence of linkage positions of the fully revolving linkage is shown.

such as the adhesive-backed PET used in the prototype shown in Fig. 1 (C and D).

The use of flexures in place of traditional pin hinges or bearings presents both challenges and possibilities for enhanced capability in developable mechanism design. Strain energy is stored in flexures during displacement. This stored energy can be used to create a preferred position to which the mechanism will return in the absence of external forces, such as the closed position in Fig. 4B. However, care must be taken in designing the stiffness of the flexures, so that the reaction forces do not deform the connected structure. Flexures only approximate revolute hinges because the location of the axis of rotation can vary slightly throughout the joints' range of motion. For a number of common compliant joints, the variation in the axis-of-rotation location has been characterized (*41*, *42*). When implementing compliant flexures into developable mechanisms, a metric such as the ratio of shortest link length to the maximum deviation from the ideal joint axis can inform the decision of whether flexures are suitable for a specific developable mechanism.

Realization: Rotatability

Flexures can create approximate revolute joints, but such joints typically have a limited range of motion. Traditional revolute joints make it possible for developable mechanisms to contain fully rotating links. In Fig. 5, we demonstrate a four-link developable mechanism placed on a generalized cylinder that has a crank link attached to a motor to create a walking motion. An explanation of the design of this mechanism is included in Materials and Methods.

DISCUSSION

Developable mechanisms show promise for use in highly constrained spaces in applications as diverse as spacecraft, automobiles, ships, architecture, furniture, clothing, construction, and medical devices. They can conform to or emerge from developable surfaces, such as aircraft fuselages and wings, submarine hulls, rocket cones, and minimally invasive surgery tools (several possible examples are shown in fig. S6). Many developable mechanisms have the possibility to be produced using existing planar manufacturing methods and then shaped into the desired surface. By defining and setting forth the fundamentals of developable mechanisms, compact mechanism design can be furthered, and additional research directions can be formalized. These include a study of the tolerance of a mechanism's functionality to misalignment between ruling lines and joint axes, integrated actuators to create or move both surface structures and the mechanisms embedded or conforming to them, topology synthesis to further integrate mechanism and structure, and special case developable mechanism synthesis such as bistable or multistable mechanisms.

The approach to defining, analyzing, and designing developable mechanisms has the ability to expand the achievable range for several mechanism performance metrics. Most notably are the metrics of mechanism volume and footprint, particularly for complex motions. Other metrics that can be potentially improved include mechanism mass, ability to stow compactly to a structure, and multifunctionality. Constrained mechanism motion volume or reach-space requirements, such as is found in sealed or pressurized environments, can be potentially addressed by considering developable mechanisms where the surface to which the mechanism conforms is a boundary for link motion.

MATERIALS AND METHODS

DH parameters for developable mechanisms

We used the DH convention to assign a frame to each link in a mechanism and specify four parameters to describe the transformation from one frame to the next. We will show how the surface geometry to which a revolute joint developable mechanism conforms can be related to these DH parameters. In addition, we will present expressions for joint offsets of revolute joints that cause the zero angle configuration, where all joint angles are zero, to coincide with the position where the developable mechanism is conforming to its associated surface.

The DH frame of the ℓ_i link, $\{i\}$, has the z axis aligned with the joint axis $\boldsymbol{z}_i$ and the x axis aligned with the common normal between joint axes $\boldsymbol{z}_{i-1}$ and $\boldsymbol{z}_i$ as shown in Fig. 6A.

Each transformation between link frames was obtained by specifying the four parameters of joint angle θ, displacement along the joint axis d, displacement along the common normal a, and twist α as shown in Fig. 6A. These four parameters were assembled into

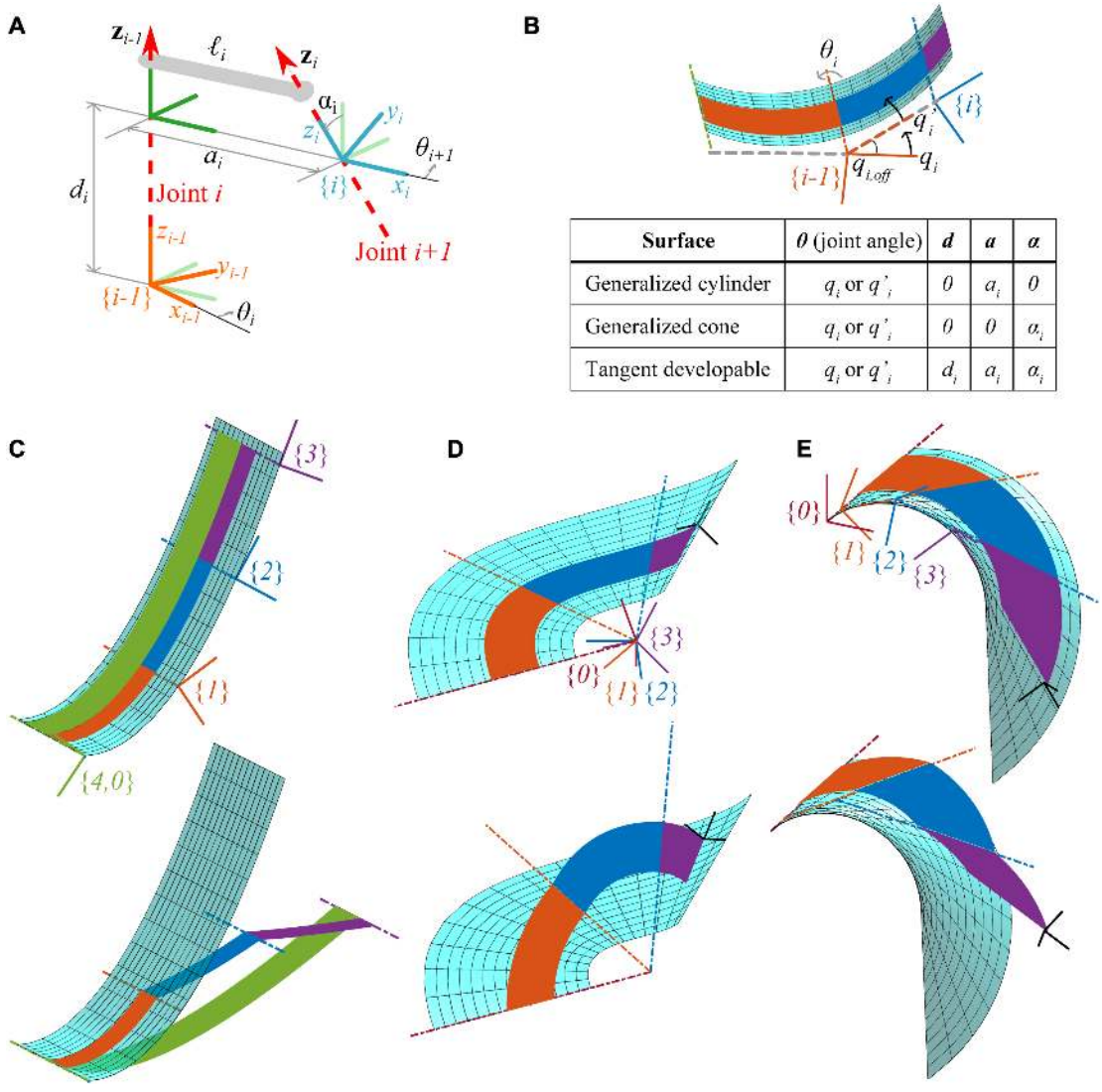

Surface	θ (joint angle)	d	a	α
Generalized cylinder	q_i or q'_i	0	a_i	0
Generalized cone	q_i or q'_i	0	0	α_i
Tangent developable	q_i or q'_i	d_i	a_i	α_i

Fig. 6. DH parameters for developable mechanisms. (**A**) DH parameter notation. (**B**) Illustration of the introduction of an offset $q_{i,\text{off}}$ at the ith revolute joint to change the zero angle reference position from the q_i axis to the q_i' axis, resulting in the zero angle position of the mechanism being the position where the links conform with the surface. The table shows which DH parameters are zero for each type of developable surface. (**C**) The DH frames on a closed-loop 4R cylindrical developable mechanism in a conforming position (top) and actuated position (bottom). (**D**) The DH frames on an open 3R chain conical developable mechanism in a conforming position (top) and actuated position (bottom). (**E**) The DH frames on an open 3R chain tangent developable mechanism in a conforming position (top) and actuated position (bottom). In (D) and (E), a possible tool frame at the end of the chain is shown in black.

a homogeneous transformation matrix from frame $\{i-1\}$ to frame $\{i\}$ as follows

$$ {}^{i-1}T_i = \begin{bmatrix} \cos\theta_i & -\sin\theta_i\cos\alpha_i & \sin\theta_i\sin\alpha_i & a_i\cos\theta_i \\ \sin\theta_i & \cos\theta_i\cos\alpha_i & -\cos\theta_i\sin\alpha_i & a_i\sin\theta_i \\ 0 & \sin\alpha_i & \cos\alpha_i & d_i \\ 0 & 0 & 0 & 1 \end{bmatrix} \quad (2) $$

For revolute joints, this transformation contains α_i, a_i, and d_i as constants and θ_i as a variable. For prismatic, or slider, joints α_i, a_i, and θ_i are constants and d_i is a variable. It is common to replace the variable in the transformation by the generalized coordinate q_i. Thus, for revolute joints, $\theta_i = q_i$, and for prismatic joints, $d_i = q_i$. This form of transformation matrix is often used with open linkage chains to compute the forward kinematics (*45*). For closed-loop linkages, we can obtain the loop-closure equations of the linkage by starting at one link frame and moving from link frame to link frame by composing the transformations until we get back to the starting link as

$$ {}^1T_2\,{}^2T_3 \ldots {}^{n-1}T_n\,{}^nT_1 = I \quad (3) $$

where n is the number of links. This produces a set of equations that describe the motion of the linkages. These equations can at times be solved analytically, but depending on the number of links and joint axis locations, numerical methods may be required.

The zero angle configuration of a linkage containing revolute joints, that is, $q_i = 0$ for $i = 1$ to n, is determined as a consequence of using DH parameters and is often not convenient or intuitive. In particular, for developable mechanisms, it is desirable to define another generalized coordinate q_i' that is offset from the previous coordinate system by a quantity $q_{i,\text{off}}$. The relationship of these coordinate systems for revolute joints is shown in Fig. 6B and is

Fig. 7. Steps for the creation of a developable mechanism, illustrated using a Chebyshev straight line mechanism integrated with a cylinder. (**A**) A cylinder with radius *R* selected as the base surface for the Chebyshev mechanism. (**B**) The ruling lines (red) that will serve as joint axes and the corresponding linkage skeleton. The ground link (ℓ_1) is dashed, while the remaining links are solid. (**C**) Applied thickness and selected link layers in the surface. (**D**) The geometry of each of the link layers, accompanied by their corresponding skeleton links, with ℓ_1 (gray), ℓ_2 (orange), ℓ_3 (purple), and ℓ_4 (blue). (**E**) The process used for defining link geometries. Motion analysis informs link shapes that avoid interference between the links. (**F**) CAD model of the developable mechanism. (**G**) Physical prototype with links labeled, demonstrating the motion of the linkage.

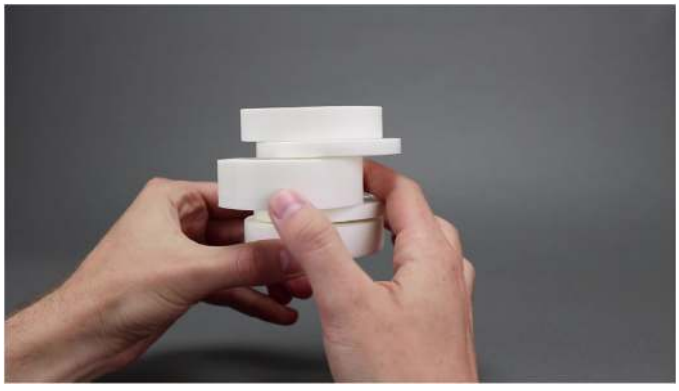

Movie 2. Movement of a Chebyshev straight line mechanism embedded in a cylinder.

Movie 3. Motorized 4R cylindrical developable mechanism. A possible walking or active-gripping motion is demonstrated.

expressed as

$$q_i = q_i' + q_{i,\text{off}} \tag{4}$$

We will present expressions for $q_{i,\text{off}}$ for revolute joints in terms of the surface geometry and DH parameters such that the zero angle configuration of a linkage in the q_i' coordinate system corresponds to the configuration where the linkage is conforming to the surface.

First, to relate the DH parameters to the geometry of the surface on which a linkage is placed, the following method was used. Let $\boldsymbol{s}(u,v)$ be a developable surface in its canonical form (*46*). This can be accomplished for the three curved developables (generalized cylinders, cones, and tangent developables) by specializing Eq. 1 by requiring $||\boldsymbol{\beta}(u)|| = 1$. Further, for generalized cylinders, $\boldsymbol{\alpha}(u)$ is orthogonal to a constant vector $\boldsymbol{\beta}$; for generalized cones, $\boldsymbol{\alpha}$ is a constant vector pointing to the apex of the cone; and for tangent developables, $\boldsymbol{\beta}(u)$ equals $\boldsymbol{\alpha}'(u)$, making $\boldsymbol{\alpha}(u)$ the edge of regression.

Although this form can represent a single generalized cylinder with the domain of v from $(-\infty,\infty)$, for generalized cones and tangent developables, this form describes two possible surfaces, one where $v \in (-\infty,0]$, which we call the reverse parametrization, and the other where $v \in [0,\infty)$, which we call the forward parametrization. To write the DH parameters using the surface geometry, we used a particular family of curves on the surface that we call cross curves. The cross curves of a developable surface are the principal curves orthogonal to the ruling lines. Given a developable surface in the form $\boldsymbol{s}(u,v)$, we can express the family of cross curves as (*46*)

$$\boldsymbol{c}(u,w) = \begin{cases} \boldsymbol{\alpha}(u) + w\boldsymbol{\beta}(u) & \text{(generalized cylinders)} \\ \boldsymbol{\alpha}(u) + w\boldsymbol{\beta}(u) \quad \text{for } w > 0 \text{ or } w < 0 & \text{(generalized cones)} \\ \boldsymbol{\alpha}(u) + s(u,w)\boldsymbol{\beta}(u) \quad \text{for } w > u \text{ or } w < u & \text{(tangent developables)} \end{cases} \tag{5}$$

where for tangent developables, $s(u,w)$ is the arc length from u to w along the edge of regression $\boldsymbol{\alpha}(u)$. We can see that, for generalized cones, the choice of the sign of w is dependent on which domain of v we have chosen for our developable surface. Likewise, for tangent developables, the condition of $w > u$ gives the cross curve for a forward parametrization, while the condition $w < u$ gives a cross curve for a reverse parametrization and results in the arc length $s(u,w)$ being negative.

It is also necessary to compute the standard unit surface normal to relate the DH parameters to the geometry. The standard unit surface normal $\mathbf{U}$ for a developable surface is independent of parameter v and given by

$$\mathbf{U}(u) = \frac{\boldsymbol{s}_u(u,v) \times \boldsymbol{s}_v(u,v)}{\|\boldsymbol{s}_u(u,v) \times \boldsymbol{s}_v(u,v)\|} \tag{6}$$

with $\boldsymbol{s}_u(u,v)$ and $\boldsymbol{s}_v(u,v)$ being the partial derivatives with respect to u and v.

We can choose which ruling lines serve as joint axes for the linkage by selecting lengths along the cross curve u_i for $i = 1$ to n, where n is the number of revolute joints. The equation for the revolute joint axis when the linkage is embedded in the surface is given by $\boldsymbol{s}(u_i,v) = v\boldsymbol{z}_{i-1}$, where $\boldsymbol{z}_{i-1}$ is the unit vector in the direction in the joint axis.

DH parameters for cylindrical developable mechanisms

For a linkage with revolute joints placed on a generalized cylinder, the DH parameters d and α are always zero, as summarized in Fig. 6B. The lengths of the common normal vectors to the joint axes, a_i, are given by

$$\boldsymbol{a}_i = \|\boldsymbol{a}_i\| \tag{7}$$

where the common normal vector is given by

$$\boldsymbol{a}_i = \boldsymbol{c}(u_{i+1}) - \boldsymbol{c}(u_i) \tag{8}$$

with $\boldsymbol{c}(u)$ being a cross curve of the generalized cylinder. For closed linkages, when $i = n$, $i + 1$ is equal to 1, completing the loop.

For open linkage chains, it is often convenient to place the first frame (attached to the grounded surface) aligned with the tangent vector to the surface and the joint axis. If this choice is made the first joint offset, $q_{1,\text{off}}$ is found using the angle between the tangent vector of a cross curve at the first joint axis and the common normal vector of the first link. The tangent vector of a cross curve at the first joint axis is $\boldsymbol{c}'(u_1)$, and $\boldsymbol{a}_1$ is computed using Eq. 8. The angle between them can be computed using the multivalued inverse tangent function [i.e., atan2(y,x)]

$$q_{1,\text{off}} = \text{atan2}((\boldsymbol{c}'(u_1) \times \boldsymbol{a}_1)\cdot\boldsymbol{z}_0, \boldsymbol{c}'(u_1)\cdot\boldsymbol{a}_1) \tag{9}$$

The remaining joint offsets for the initial configuration $q_{i,\text{off}}$ for $i > 1$ can be found by calculating the angle between two sequential common normal vectors using Eq. 9 with $\boldsymbol{a}_{i-1}$, $\boldsymbol{a}_i$, and $\boldsymbol{z}_{i-1}$ instead of $\boldsymbol{c}'(u_1)$, $\boldsymbol{a}_1$, and $\boldsymbol{z}_0$, which results in

$$q_{i,\text{off}} = \text{atan2}((\boldsymbol{a}_{i-1} \times \boldsymbol{a}_i) \cdot \boldsymbol{z}_{i-1}, \boldsymbol{a}_{i-1} \cdot \boldsymbol{a}_i) \tag{10}$$

For closed linkages, we can use Eq. 10, where for $i = 1$, $i - 1 = n$, to complete the linkage loop. An example of a closed-loop 4R cylindrical developable mechanism placed on a half parabolic surface is shown in Fig. 6C in conforming and actuated positions. The DH frames were labeled where the color of the frame corresponds to the color of the link to which it is attached. The ground link that is integrated with the surface is the orange link with DH frame {1}.

DH parameters for conical developable mechanisms

The DH parameters for a generalized cone with a linkage with revolute joints placed on it are summarized in Fig. 6B, where d and a are always zero. The twists can be calculated as

$$\begin{aligned} \alpha_i &= \text{atan2}(\|\boldsymbol{z}_{i-1} \times \boldsymbol{z}_i\|, \boldsymbol{z}_{i-1} \cdot \boldsymbol{z}_i) \quad \text{for forward parametrizations } v \in [0, \infty) \\ \alpha_i &= \text{atan2}(-\|\boldsymbol{z}_{i-1} \times \boldsymbol{z}_i\|, \boldsymbol{z}_{i-1} \cdot \boldsymbol{z}_i) \text{ for reverse parametrizations } v \in (-\infty, 0] \end{aligned} \tag{11}$$

For open linkages with the first frame aligned with the tangent to the surface and the $\boldsymbol{z}_0$ joint axis, the first joint offset, $q_{1,\text{off}}$, is

$$q_{1,\text{off}} = \text{atan2}((\mathbf{U}(u_1) \times \boldsymbol{N}_1) \cdot \boldsymbol{z}_0, \mathbf{U}(u_1) \cdot \boldsymbol{N}_1) + \pi/2 \tag{12}$$

where $\boldsymbol{N}_1 = -(\boldsymbol{z}_0 \times \boldsymbol{z}_1)$ for a forward parametrization or $\boldsymbol{N}_1 = (\boldsymbol{z}_0 \times \boldsymbol{z}_1)$ for a reverse parametrization. The remaining joint offsets, $q_{i,\text{off}}$ for $i > 1$, are found from the angle given by

$$q_{i,\text{off}} = \text{atan2}((\boldsymbol{N}_i \times \boldsymbol{N}_{i+1}) \cdot \boldsymbol{z}_{i-1}, \boldsymbol{N}_i \cdot \boldsymbol{N}_{i+1}) \tag{13}$$

where $\boldsymbol{N}_i = \boldsymbol{z}_{i-2} \times \boldsymbol{z}_{i-1}$. This same formula can be used for closed linkages, where when $i = 1$, $\boldsymbol{z}_{i-2} = \boldsymbol{z}_{n-1}$.

An open linkage conical developable mechanism is shown in Fig. 6D in conforming and actuated positions. The DH frames shown on the conforming position show how the frames are concentrated at the focal point of the generalized cone.

DH parameters for tangent developable mechanisms

The DH parameters for a linkage with revolute joints on tangent developable surfaces are summarized in Fig. 6B. Unlike generalized cones and cylinders, tangent developables allow skew joint axes, so none of the DH parameters simplifies to zero.

We can draw upon methodology created for writing spatial mechanisms in DH convention to calculate these parameters. We refer the reader to the method presented in (*29*) to calculate the parameters d_i, α_i, and a_i.

For an open linkage with the first frame aligned with the joint axis and tangent to the surface, the first joint offset, $q_{1,\text{off}}$, is found by

$$q_{1,\text{off}} = \text{atan2}((\mathbf{U}(u_1) \times \boldsymbol{N}_1) \cdot \boldsymbol{z}_0, \mathbf{U}(u_1) \cdot \boldsymbol{N}_1) - \pi/2 \tag{14}$$

where $\mathbf{U}(u_1)$ is the surface normal at the first joint axis and $\boldsymbol{N}_1$ is the vector orthogonal to $\boldsymbol{z}_0$ and $\boldsymbol{z}_1$ such that a_1 is positive along this vector [see (*29*) for more details on the direction of $\boldsymbol{N}_1$]. The remaining joint offsets are found using

$$q_{i,\text{off}} = \text{atan2}((\boldsymbol{N}_{i-1} \times \boldsymbol{N}_i) \cdot \boldsymbol{z}_{i-1}, \boldsymbol{N}_{i-1} \cdot \boldsymbol{N}_i) \tag{15}$$

where $\boldsymbol{N}_i$ is orthogonal to $\boldsymbol{z}_{i-2}$ and $\boldsymbol{z}_{i-1}$ such that a_i is positive along the vector. This same formula is used for closed linkages where if $i = 1$, then $\boldsymbol{z}_{i-2} = \boldsymbol{z}_{n-1}$. An open linkage 3R tangent developable mechanism is shown in Fig. 6E in conforming and actuated positions.

Prototyping and design methods

The mechanisms presented in Figs. 2 (D, E, I, J, N, and O), 3F, and 5 were modeled using computer-aided design (CAD) and then additively manufactured via fused deposition modeling and stereolithography techniques with polylactic acid and photopolymer resin, respectively. The compliant mechanism in Fig. 4B was also modeled in CAD and then cut out by water jet from a 1-mm-thick 6061 aluminum sheet that was first adhered to a 6.4-mm ABS sheet backing using 3M Super 77 Multipurpose Adhesive.

Design of a Chebyshev linkage contained in a cylinder

A Chebyshev linkage contained in a right cylinder was constructed to further demonstrate the steps to create a developable mechanism. The Chebyshev linkage was created by Chebyshev (*47*) in the 19th century and is known for its ability to create an approximate straight line motion for a point on the coupler link from rotatory motion input (see fig. S7A). Details for each step to embed this mechanism into a cylinder are described below.

First, the zero-thickness developable surface of a right cylinder was selected as the surface in which the mechanism was to be embedded, as shown in Fig. 7A. This cylinder is represented by the parametric surface, where the directrix, $\boldsymbol{\alpha}(u)$, is the equation of a circle in the xy plane and the ruling lines are in the z direction, $\boldsymbol{\beta}(v)$, giving

$$\boldsymbol{s}(u, v) = \begin{bmatrix} R\cos(u) \\ R\sin(u) \\ 0 \end{bmatrix} + v \begin{bmatrix} 0 \\ 0 \\ 1 \end{bmatrix} \tag{16}$$

where R is the radius of the cylinder and $u \in [0, 2\pi]$.

Second, the joint axes for a Chebyshev linkage correspond to the lines $\boldsymbol{s}(u_i, v)$, where $u_1 = 5.601$ (320.9°), $u_2 = 3.824$ (219.1°), $u_3 = 1.172$ (67.2°), and $u_4 = 1.969$ (112.8°). These axis lines create link-length ratios of $L_1 : L_2 : L_3 : L_4 = 2 : 2.5 : 1 : 2.5$, as shown in Fig. 7B. The ratio of the cylinder's radius to these link lengths can be computed to be $R/L_3 = \sqrt{1 + \left(\frac{13}{16}\right)^2} \approx 1.288$.

Third, the kinematic equations of the Chebyshev linkage have been well studied through a variety of methods, and here, a general method of using DH parameters to find the loop-closure equations will be demonstrated. The DH parameters for this linkage are found by first writing the equation of a cross curve for the developable surface from $\boldsymbol{s}(u, v)$. For simplicity, $w = 0$ is

chosen, resulting in

$$\boldsymbol{c}(u) = \begin{bmatrix} R\cos(u) \\ R\sin(u) \\ 0 \end{bmatrix} \quad (17)$$

From the cross curve, Eq. 7 was used to write the lengths of the common normals, a_i, which correspond to the link-length ratios previously given in terms of the radius of the circle as $a_1 = R(1.552)$, $a_2 = a_4 = R(1.940)$, and $a_3 = R(0.776)$. The joint angles θ_i were assigned to be generalized coordinates q_i because each joint is revolute. Furthermore, since d and α are zero for generalized cylinders, this provides all the information needed to write the homogeneous transformation matrices using Eq. 2 (see fig. S7B for the DH frames on the Chebyshev straight line mechanism skeleton). Equation 3 is then used to find the loop-closure equations. This results in 16 equations, where 10 are identities, 4 yield an equivalent unique result, and the remaining 2 equations are unique. This system of three unique equations can be simplified to

$$\begin{gathered} \sin(q_1 + q_2 + q_3 + q_4) = 0 \\ a_1 + a_2\cos(q_2) + a_3\cos(q_2 + q_3) + a_4\cos(q_1) = 0 \\ a_2\sin(q_2) + a_3\sin(q_2 + q_3) - a_4\sin(q_1) = 0 \end{gathered} \quad (18)$$

By designating one of the joint angles q as a known input link, the system can be solved numerically to find the other three unknown joint angles. The system was solved using a nonlinear constrained solver (fmincon in MATLAB), where q_3 was selected as the known input link because it has a one-to-one mapping with the other angles when q_1 and q_2 are constrained to the region from $[\pi, 2\pi]$.

Next, Eq. 10 was used to find the joint offsets for the initial linkage configuration that was embedded in the cylindrical surface as $q_{1,\text{off}} = q_{2,\text{off}} = -2.214$ (−126.9°) and $q_{3,\text{off}} = q_{4,\text{off}} = 2.214$(126.9°). With Eq. 4, the solved joint angles q_i were transformed to the q_i' frames (see fig. S7C for a plot of the q' joint angle relationships). With the joint angles known, the motion of any point on the links can be tracked. This was done for the path of the point midway between joint axes $\boldsymbol{z}_2$ and $\boldsymbol{z}_3$ (see the brown curve in fig. S7A). A portion of this path includes the classic nearly straight line motion produced by the Chebyshev linkage.

Fourth, this mechanism is intended to be contained in the surface, so thickness was added symmetrically about the zero-thickness model as shown in Fig. 7C. Fifth and last, the link shapes were defined to be contained in the surface with the linkage motion analysis further informing the geometry for interference prevention. For this Chebyshev linkage on a cylinder, interference between adjacent moving links was mitigated by selecting layers for each moving link as shown by the colored bands in Fig. 7C. The ground link (ℓ_1), shown in gray, connects to both sides of the moving link layers, so there must be a continuous path through all the layers for the ground link. Figure 7D shows each layer, beginning with the full-cylinder ground link and the arrangement of the link geometries and ground link in each subsequent layer. The extreme ranges of motion of ℓ_2 are shown in Fig. 7E in light orange. Considerable freedom exists in choosing the position of the black dot separating ℓ_1 and ℓ_2. The interference-preventing cut containing this point follows a circular arc with a center at the joint axis $\boldsymbol{z}_1$. Similar steps were used for ℓ_4. ℓ_3, the coupler, is shaped by using the nearly straight line motion of the midpoint of the skeletal diagram link shown by the black dot and path shown in brown in Fig. 7E. Considering this dot as the center of the light purple circle that rolls along the flat gray region, the shape of ℓ_3 avoids interference by staying within the circle. The radius of the light purple circle can be adjusted. A video of the motion of this mechanism can be seen in Movie 2.

Design of a motorized 4R cylindrical developable mechanism

The motorized 4R in Fig. 5 was created using the steps described for the 4R cylindrical developable mechanism (see fig. S1 and descriptions in Supplementary Text) with some differences. ℓ_2 was mirrored across ℓ_3 for added stability. Features were also incorporated into the cylindrical surface for motor and gear mounting. Special care was taken to ensure that the joint between ℓ_2 and ℓ_3 does not interfere with the motor body while fully revolving. The link lengths were otherwise arbitrarily selected. A video of the motion of this mechanism can be seen in Movie 3.

SUPPLEMENTARY MATERIALS

robotics.sciencemag.org/cgi/content/full/4/27/eaau5171/DC1

Text

Fig. S1. Steps for the creation of a cylindrical developable mechanism.

Fig. S2. Labels for the Bennett linkage mobility criteria.

Fig. S3. Steps for the creation of a tangent developable mechanism.

Fig. S4. Labels for the dimensions of the fundamental unit of the outside LET joint used in the compliant 4R.

Fig. S5. The rolling process used to make the compliant cylindrical 4R.

Fig. S6. Examples of possible developable mechanisms incorporated into cylindrical systems.

Fig. S7. Chebyshev linkage.

Table S1. The dimensions of the fundamental unit used in the compliant 4R.

Reference (*48*)

REFERENCES AND NOTES

1. V. Megaro, J. Zehnder, M. Bächer, S. Coros, M. Gross, B. Thomaszewski, A computational design tool for compliant mechanisms. *ACM Trans. Graph.* **36**, 82 (2017).
2. A. G. Dunning, N. Tolou, J. L. Herder, A compact low-stiffness six degrees of freedom compliant precision stage. *Precis. Eng.* **37**, 380–388 (2013).
3. T. Q. Trung, N.-E. Lee, Recent progress on stretchable electronic devices with intrinsically stretchable components. *Adv. Mater.* **29**, 1603167 (2016).
4. J. O. Jacobsen, B. G. Winder, L. L. Howell, S. P. Magleby, Lamina emergent mechanisms and their basic elements. *J. Mech. Robot.* **2**, 011003 (2009).
5. P. S. Gollnick, S. P. Magleby, L. L. Howell, An introduction to multilayer lamina emergent mechanisms. *J. Mech. Des.* **133**, 081006 (2011).
6. S. Felton, M. Tolley, E. Demaine, D. Rus, R. Wood, A method for building self-folding machines. *Science* **345**, 644–646 (2014).
7. H. Fu, K. Nan, W. Bai, W. Huang, K. Bai, L. Lu, C. Zhou, Y. Liu, F. Liu, J. Wang, M. Han, Z. Yan, H. Luan, Y. Zhang, Y. Zhang, J. Zhao, X. Cheng, M. Li, J. W. Lee, Y. Liu, D. Fang, X. Li, Y. Huang, Y. Zhang, J. A. Rogers, Morphable 3D mesostructures and microelectronic devices by multistable buckling mechanics. *Nat. Mater.* **17**, 268–276 (2018).
8. Y. Chen, R. Peng, Z. You, Origami of thick panels. *Science* **349**, 396–400 (2015).
9. J. A. Faber, A. F. Arrieta, A. R. Studart, Bioinspired spring origami. *Science* **359**, 1386–1391 (2018).
10. A. E. Marras, L. Zhou, H.-J. Su, C. E. Castro, Programmable motion of DNA origami mechanisms. *Proc. Natl. Acad. Sci. U.S.A.* **112**, 713–718 (2015).
11. K. Zhang, Y. H. Jung, S. Mikael, J.-H. Seo, M. Kim, H. Mi, H. Zhou, Z. Xia, W. Zhou, S. Gong, Z. Ma, Origami silicon optoelectronics for hemispherical electronic eye systems. *Nat. Commun.* **8**, 1782 (2017).
12. X. Ma, K. Zhang, J. S. Dai, Novel spherical-planar and Bennett-spherical 6R metamorphic linkages with reconfigurable motion branches. *Mech. Mach. Theory* **128**, 628–647 (2018).
13. M. Salerno, K. Zhang, A. Menciassi, J. S. Dai, A novel 4-DOF origami grasper with an SMA-actuation system for minimally invasive surgery. *IEEE Trans. Robot.* **32**, 484–498 (2016).
14. K. Zhang, C. Qiu, J. S. Dai, An extensible continuum robot with integrated origami parallel modules. *J. Mech. Robot.* **8**, 031010 (2016).

15. M. Johnson, Y. Chen, S. Hovet, S. Xu, B. Wood, H. Ren, J. Tokuda, Z. T. H. Tse, Fabricating biomedical origami: A state-of-the-art review. *Int. J. Comput. Assist. Radiol. Surg.* **12**, 2023–2032 (2017).
16. V. A. Bolaños Quiñones, H. Zhu, A. A. Solovev, Y. Mei, D. H. Gracias, Origami biosystems: 3D assembly methods for biomedical applications. *Adv. Biosys.* **2**, 1800230 (2018).
17. L. E. Torfason, F. R. E. Crossley, Use of the intersection of surfaces as a method for design of spatial mechanisms, in *3rd World Congress for the Theory of Machines and Mechanisms* (Kupari, Yugoslavia, 1971), vol. B., pp. 247–258.
18. P. C. López-Custodio, J. Dai, J. Rico, Branch reconfiguration of Bricard linkages based on toroids intersections: Line-symmetric case. *J. Mech. Robot.* **10**, 31002 (2018).
19. D. J. Struik, *Lectures on Classical Differential Geometry* (Addison-Wesley Pub. Co., Reading, 1961).
20. C. Tang, P. Bo, J. Wallner, H. Pottmann, Interactive design of developable surfaces. *ACM Trans. Graph.* **35**, 12 (2016).
21. M. Kilian, A. Monszpart, N. J. Mitra, String actuated curved folded surfaces. *ACM Trans. Graph.* **36**, 1–13 (2017).
22. K. H. Hunt, *Kinematic Geometry of Mechanisms* (Oxford Univ. Press, 1978), vol. 7.
23. L.-T. Schreiber, C. Gosselin, Kinematically redundant planar parallel mechanisms: Kinematics, workspace, and trajectory planning. *Mech. Mach. Theory* **119**, 91–105 (2018).
24. X. Zhao, H. Liu, H. Ding, L. Qian, An approach for computing the transmission index of full mobility planar multiloop mechanisms. *J. Mech. Robot.* **9**, 041017 (2017).
25. V. Venkataramanujam, P. M. Larochelle, Design and development of planar reconfigurable motion generators. *Mech. Based Des. Struct. Mach.* **44**, 426–439 (2016).
26. C. H. Chiang, *Kinematics of Spherical Mechanisms* (Krieger Publishing, 2000).
27. G. Wei, J. S. Dai, Origami-inspired integrated planar-spherical overconstrained mechanisms. *J. Mech. Des.* **136**, 051003 (2014).
28. J. Landuré, C. Gosselin, Kinematic analysis of a novel kinematically redundant spherical parallel manipulator. *J. Mech. Robot.* **10**, 021007 (2018).
29. J. M. McCarthy, G. S. Soh, *Geometric Design of Linkages* (Springer Science & Business Media, 2010), vol. 11.
30. J. Phillips, *Freedom in Machinery* (Cambridge Univ. Press, 1990), vol. 2.
31. X. Kong, Geometric construction and kinematic analysis of a 6R single-loop overconstrained spatial mechanism that has three pairs of revolute joints with intersecting axes. *Mech. Mach. Theory* **102**, 196–202 (2016).
32. F. P. Rad, R. Vertechy, G. Berselli, V. Parenti-Castelli, Analytical compliance analysis and finite element verification of spherical flexure hinges for spatial compliant mechanisms. *Mech. Mach. Theory* **101**, 168–180 (2016).
33. H. Pottmann, J. Wallner, *Computational Line Geometry* (Springer, 2010).
34. G. T. Bennett, A new mechanism. *Engineering* **76**, 777–778 (1903).
35. D. Lei, A. E. Marras, J. Liu, C.-M. Huang, L. Zhou, C. E. Castro, H.-J. Su, G. Ren, Three-dimensional structural dynamics of DNA origami Bennett linkages using individual-particle electron tomography. *Nat. Commun.* **9**, 592 (2018).
36. Z. Xie, L. Qiu, D. Yang, Design and analysis of Outside-Deployed Lamina Emergent Joint (OD-LEJ). *Mech. Mach. Theory* **114**, 111–124 (2017).
37. B. G. Winder, S. P. Magleby, L. L. Howell, Kinematic representations of pop-up paper mechanisms. *J. Mech. Robot.* **1**, 021009 (2009).
38. Z. You, Y. Chen, *Motion Structures* (Spon Press, 2012).
39. E. Abbena, S. Salamon, A. Gray, *Modern Differential Geometry of Curves and Surfaces with Mathematica* (CRC Press, 2017).
40. R. S. Hartenberg, Scheunemann, J. Denavit, *Kinematic Synthesis of Linkages* (McGraw-Hill, 1964).
41. L. L. Howell, *Compliant Mechanisms* (John Wiley & Sons, 2001).
42. L. L. Howell, S. P. Magleby, B. M. Olsen, *Handbook of Compliant Mechanisms* (Wiley, 2013).
43. V. K. Venkiteswaran, H.-J. Su, Pseudo-rigid-body models for circular beams under combined tip loads. *Mech. Mach. Theory* **106**, 80–93 (2016).
44. J. O. Jacobsen, G. Chen, L. L. Howell, S. P. Magleby, Lamina emergent torsional (LET) joint. *Mech. Mach. Theory* **44**, 2098–2109 (2009).
45. P. Corke, *Robotics, Vision & Control* (Springer, 2017).
46. R. J. Lang, T. G. Nelson, S. P. Magleby, L. L. Howell, Kinematics and discretization of curved-fold mechanisms, paper no. DETC2017-67439 in *ASME 2017 International Design Engineering Technical Conferences and Computers and Information in Engineering Conference* (ASME, 2017).
47. P. L. Chebyshev, *Oeuvres de PL Tchebychef* (Commissionaires de l'Académie impériale des sciences, 1899), vol. 1.
48. J. E. Shigley, *Shigley's Mechanical Engineering Design* (Tata McGraw-Hill Education, 2011).

Acknowledgments: We thank B. Reneer for illustration expertise. **Funding:** This work was supported by the U.S. National Science Foundation through NSF grant no. 1663345 and NSF Graduate Research Fellowship Program under grant no. 1247046. **Author contributions:** All authors contributed to the conceptualization and methodology. T.K.Z., T.G.N., and L.L.H. were primary contributors to the writing and editing of the manuscript. T.K.Z. and T.G.N. were primary contributors for visualization. **Competing interests:** T.G.N., L.L.H., and S.P.M. are inventors on a patent application (provisional application no. 62685568) related to the content of this paper. All other authors declare that they have no competing interests. **Data and materials availability:** All data needed to evaluate the conclusions in the paper are present in the paper and/or Supplementary Materials.

Submitted 18 June 2018
Accepted 12 December 2018
Published 13 February 2019
10.1126/scirobotics.aau5171

Citation: T. G. Nelson, T. K. Zimmerman, S. P. Magleby, R. J. Lang, L. L. Howell, Developable mechanisms on developable surfaces. *Sci. Robot.* **4**, eaau5171 (2019).

Developable mechanisms on developable surfaces

Todd G. Nelson, Trent K. Zimmerman, Spencer P. Magleby, Robert J. Lang and Larry L. Howell

Sci. Robotics **4**, eaau5171.
DOI: 10.1126/scirobotics.aau5171